Acta Crystallographica Section A
Foundations of Crystallography
ISSN 0108-7673

Received 6 March 2012
Accepted 19 April 2012

On the optical theorem applicability using a self-consistent wave approximation model for the grazing-incidence small-angle X-ray scattering from rough surfaces

F. N. Chukhovskii

Institute of Crystallography, Russian Academy of Sciences, Leninsky Prospect 59, 119333 Moscow, Russian Federation. Correspondence e-mail: tschoukhowski@hotmail.com

Based on a self-consistent wave approximation (SCWA) for describing the grazing-incidence small-angle X-ray scattering (GISAXS) from a random rough surface, the optical theorem applicability is tested. Asymptotic solutions for the specular and diffuse GISAXS waves are used to evaluate the X-ray energy flows through the planes far away from the surface interface, $z \rightarrow \pm\infty$. The conventional Fresnel expressions multiplied by the corresponding Debye–Waller factors are used for the specular waves, while the diffuse X-ray energy flows are described in terms of the product of the statistical scattering factors $\eta_R(\theta, \theta_0)$ and $\eta_T(\theta, \theta_0)$ and the Fourier transform of the two-point cumulant correlation function $g_2(|\mathbf{x}_1 - \mathbf{x}_2|/\ell)$ (θ is the grazing scattering angle with the surface, φ is the azimuth scattering angle; θ_0 is the grazing-incidence angle). It is shown that the optical theorem within the SCWA does hold in the case of infinite correlation lengths $\ell \rightarrow \infty$ (more precisely, $k\ell\theta_0^2 >> 1$, k is the X-ray wavenumber in a vacuum). In a general case of the typical-valued $\{\theta_0, \sigma, \ell\}$ parameters the reflected and transmitted GISAXS wave flows are numerically integrated over the scattering reciprocal space to probe the optical theorem.

© 2012 International Union of Crystallography
Printed in Singapore – all rights reserved

1. Introduction

As is well known, grazing-incidence small-angle X-ray scattering (GISAXS) is a unique tool for the non-destructive characterization of solid/liquid medium surfaces and layered structures with a thickness in the mesoscopic range of lengths from a few nanometres up to some micrometres. It is particularly important for investigating the self-organized formation of semiconductor nanostructures (see, *e.g.*, Pietsch *et al.*, 2004; Schmidbauer *et al.*, 2008; Renaud *et al.*, 2009 and references therein); it has proved to be very effective for the non-destructive characterization of semiconductor quantum dots and wires (Schmidbauer *et al.*, 2008). In particular, the electron density of epitaxic SiGe nano-islands has been investigated in depth using coherent GISAXS (Zozulya *et al.*, 2008).

Most of the experimental and theoretical works to date have been concerned with specular GISAXS, which has been mainly interpreted in terms of the conventional Fresnel coefficients multiplied by the corresponding Debye–Waller factors. The latter are exponential factors and quadratically depend on the root-mean-square (r.m.s.) roughness σ of a random rough interface (the well known Debye–Waller approach; see, *e.g.*, Nevot & Croce, 1980; Sinha *et al.*, 1988; de Boer, 1994, 1995; Lazzari, 2002; Chukhovskii, 2009).

An attempt to go beyond the Debye–Waller approximation for specular GISAXS and take into account the X-ray multiple-scattering effects has been made by Chukhovskii & Polyakov (2010).

The diffuse reflectivity scan $R_{\rm dif}(\theta, \varphi; \theta_0)$ is particularly informative and can be recorded in the angular range $\{\theta, \varphi\}$ with necessary resolution at the given grazing-incidence angle θ_0 (θ is the scattering angle with the surface and φ is the scattering azimuth angle).

Note that the conventional Born approximation is invalid to describe the diffuse scan $R_{\rm dif}(\theta, \varphi; \theta_0)$. In particular, in its framework one cannot explain Yoneda's peak of the diffuse scan $R_{\rm dif}(\theta, \varphi; \theta_0)$ experimentally observed at scattering angles θ very close to $\theta_{\rm cr}$, the critical angle of incidence for total external reflection (Yoneda, 1963). Instead, the distorted-wave Born approximation (DWBA) is required to solve the integral wave equation and correctly describe the GISAXS wave propagation through a rough interface of vacuum and medium (Petrashen' *et al.*, 1983; Vinogradov *et al.*, 1985; Sinha *et al.*, 1988).

The reverse issue of retrieving physical parameters such as, in particular, the medium density [associated with the critical angle $\theta_{\rm cr} = (-{\rm Re}\,\chi)^{1/2}$], the r.m.s. roughness σ, and the two-point cumulant correlation function $g_2(|\mathbf{x}_1 - \mathbf{x}_2|/\ell)$ from experimental and specular, $R_{\rm spec}(\theta, \theta_0)$, and diffuse,

$R_{\rm dif}(\theta,\ \varphi;\ \theta_0)$, data is a good challenge for the GISAXS theory.

Clearly, the relevant scattering theory for describing the GISAXS from rough surfaces is of special significance. As pointed out by Sinha *et al.* (1988), the basic manifestation of the GISAXS theory is the optical theorem, which is nothing other than the energy conservation law. Unfortunately, it does not hold within the DWBA. Recently, applying the perturbation theory in order to solve the integral wave equation (IWE), the optical theorem applicability has been investigated by Kozhevnikov (2010). It was proved that the optical theorem holds provided that the diffuse GISAXS can be evaluated in the first-order DWBA, while for the specular GISAXS the IWE solution should be determined up to the second-order DWBA inclusively.

On the other hand, the implementation of the optical theorem is still open for relatively large values of the r.m.s. roughness parameter σ, when the perturbation theory cannot be applied.

In this paper, which aims to go beyond the DWBA method, the Green function formalism is applied to analyse the optical theorem applicability based on a self-consistent wave approximation (SCWA) proposed in Chukhovskii (2011).

The paper is organized as follows: in §2 we shall use the Green function (point-source) formalism to convert the stationary wave equation to the integral form. The kernel function of the Green function compound represents by itself the bilinear superposition of the two standard Fresnel solutions of the GISAXS from the flat surface. In §3, we will use the SCWA to analytically derive asymptotic solutions for the X-ray wavefield propagating within a vacuum and medium far away from the rough surface interface $z \to \pm\infty$. In §4, the Gaussian model to statistically describe a random rough surface in terms of the r.m.s. interface roughness σ and two-point cumulant correlation function $g_2(|\mathbf{x}_1 - \mathbf{x}_2|/\ell)$ is utilized. Further, within the Gaussian statistics the analytical expressions for the statistical scattering factor $\eta_{\rm R}(\theta, \theta_0)$ and $\eta_{\rm T}(\theta, \theta_0)$ related to diffuse reflection and transmission flows, $R_{\rm dif}(\theta,\ \varphi;\ \theta_0)$ and $T_{\rm dif}(\theta,\ \varphi;\ \theta_0)$, are derived, whereas the conventional Debye–Waller factors for the specular ones, $R_{\rm spec}(\theta, \theta_0)$ and $T_{\rm spec}(\theta, \theta_0)$, are obtained.

Specifically, following Kozhevnikov (2010), the optical theorem is formulated in the form of equality of the X-ray energy flows through two parallel planes for $z \to \pm\infty$ in the case of a non-absorbing medium, Im χ = 0.

We shall show that the optical theorem within the SCWA is strictly satisfied in the case of infinite two-point correlation lengths $\ell \to \infty$, more precisely $k\ell\theta_0^{\,2} \gg 1$, where $k = |\mathbf{k}_0|$ is the X-ray wavenumber in a vacuum.

In §5, to probe the optical theorem applicability for the typical-valued parameter array of $\{\theta_0,\ \sigma,\ \ell\}$, the diffuse reflection and transmission flows, $R_{\rm dif}(\theta,\ \varphi;\ \theta_0)$ and $T_{\rm dif}(\theta,\ \varphi;\ \theta_0)$, are integrated over the whole angular range $(\theta,\ \varphi)$.

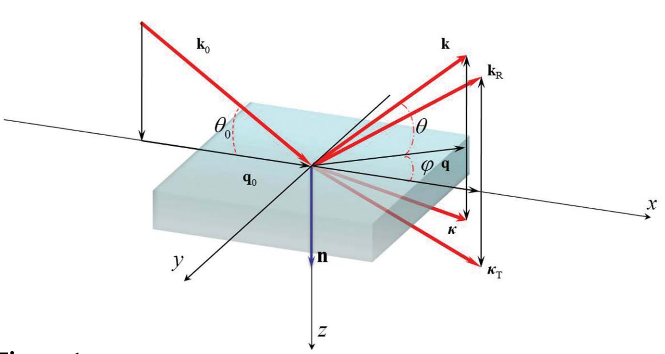

Figure 1
GISAXS layout: $\mathbf{k}_0 = \mathbf{q}_0 + k_z\mathbf{n}$ is the incident wavevector, $\mathbf{k}_{\rm R} = \mathbf{q}_0 - k_z\mathbf{n}$ and $\boldsymbol{\kappa}_{\rm T} = \mathbf{q}_0 + \kappa_z\mathbf{n}$ are the wavevectors of the specular reflected and transmitted waves, respectively; $\mathbf{k} = \mathbf{q} - k_z(q)\mathbf{n}$ and $\boldsymbol{\kappa} = \mathbf{q} + \kappa_z(q)\mathbf{n}$ are the wavevectors of the reflected and transmitted diffuse waves, respectively; $\mathbf{n}$ is the unit vector along the z direction perpendicular to the average flat surface z = 0.

2. Integral wave equation. The Green function formalism

With the aim of introducing the necessary mathematical formalism, we will briefly repeat the theoretical problem analysis up to equation (10) given in Chukhovskii (2011).

Let the incident X-ray plane wave $E_{\rm inc}(\mathbf{r}) = \exp(i\mathbf{k}_0\mathbf{r})$ impinge on a rough interface that separates a vacuum and medium, where $\mathbf{k}_0 = \mathbf{q}_0 + k_z\mathbf{n}$ is the incident wavevector, $\mathbf{q}_0$ is the lateral wavevector component and $k_z = (k^2 - \mathbf{q}_0^{\,2})^{1/2}$ is the internal-normal wavevector component along the z direction perpendicular to the averaged flat surface z = 0, $k = |\mathbf{k}_0|$ is the wavenumber in a vacuum (see Fig. 1).

The TE-polarized X-ray wavefield component is assumed to be under consideration. Recall that in the case of the GISAXS TM-polarized X-rays for grazing incidence the results are the same as for TE polarization (see, *e.g.*, Sinha *et al.*, 1988). For reference, the X-ray wavelength λ is of the order of 0.1 nm, the complex electric susceptibility $\chi \equiv {\rm Re}\,\chi + i{\rm Im}\,\chi$, ${\rm Re}\,\chi < 0$ and ${\rm Im}\,\chi > 0$. In the case of interest the X-ray wavelength λ is of the order of 0.1 nm, ${\rm Re}\,\chi \sim -10^{-5}$ and ${\rm Im}\,\chi \sim 0.05|{\rm Re}\,\chi|$ are assumed.

In the case under consideration, the stationary wave equation describes the GISAXS of a TE-polarized wavefield propagating through a rough interface between a vacuum and medium,

$$\{\nabla^2 + k^2[1 + \chi\Theta(z)]\}E(\mathbf{r}) = -k^2\delta\chi(\mathbf{r})E(\mathbf{r}), \qquad (1)$$

where $E(\mathbf{r})$ is the wavefunction for a TE-polarized electric wavefield and the electric susceptibility deviation $\delta\chi(\mathbf{r})$ has the form

$$\delta\chi(\mathbf{r}) = \chi\{\Theta[z - h(\mathbf{x})] - \Theta(z)\}. \qquad (2)$$

$h(\mathbf{x})$ is the height of an actual rough surface at the point $\mathbf{x}$ (assumed to be single valued); $\Theta(z)$ is the unit step function: $\Theta(z) = 0$ for $z < 0$ and $\Theta(z) = 1$ for $z > 0$.

According to the basic idea of the Green function formalism, equation (1) can be converted into the IWE (*cf.* Vinogradov *et al.*, 1985; Kozhevnikov, 2010; Chukhovskii, 2011):

$$E(\mathbf{r}) = E_0(\mathbf{r}) - k^2 \int {\rm d}^3\mathbf{r}'\, \mathbf{G}(\mathbf{r}, \mathbf{r}')\Delta\chi(\mathbf{r}')E(\mathbf{r}'). \qquad (3)$$

Herein, the Green (point-source) function $\mathbf{G}(\mathbf{r}, \mathbf{r}')$ is defined by

$$\begin{aligned}\mathbf{G}(\mathbf{r}, \mathbf{r}') = -i(4\pi)^{-2} \textstyle\int \mathrm{d}^2\mathbf{q}\,[k_z^{-1}(q) + \kappa_z^{-1}(q)] \\ \times \exp[i\mathbf{q}(\mathbf{x} - \mathbf{x}')]\begin{cases} y_2(z, q)y_1(z', q), & z \le z' \\ y_1(z, q)y_2(z', q), & z \ge z' \end{cases}\end{aligned} \quad (4)$$

in the twofold medium with the step-like abrupt electric susceptibility $\chi(\mathbf{r}) = \chi\Theta(z)$.

Functions $y_1(z, q)$ and $y_2(z, q)$ are the two eigenfunctions of the stationary wave equation

$$\mathrm{d}^2y/\mathrm{d}z^2 + \{k^2[1 + \chi\Theta(z)] - q^2\}y = 0 \quad (5)$$

along the z direction and then they represent by themselves the standard Fresnel solutions

$$\begin{aligned} y_1(z, q) &= \begin{cases} \exp[ik_z(q)z] + R_1(q)\exp[-ik_z(q)z] & \text{for } z \le 0 \\ T_1(q)\exp[i\kappa_z(q)z] & \text{for } z \ge 0 \end{cases} \\ y_2(z, q) &= \begin{cases} T_2(q)\exp[-ik_z(q)z] & \text{for } z \le 0 \\ \exp[-i\kappa_z(q)z] + R_2(q)\exp[i\kappa_z(q)z] & \text{for } z \ge 0 \end{cases} \end{aligned} \quad (6)$$

in the direct and mirror-reversed GISAXS geometry, respectively.

The reflection, $R_1(q)$ and $R_2(q)$, and transmission, $T_1(q)$ and $T_2(q)$, coefficients take the standard Fresnel form

$$\begin{aligned} R_1(q) &= \frac{k_z(q) - \kappa_z(q)}{k_z(q) + \kappa_z(q)} \quad \text{and} \quad R_2(q) = \frac{\kappa_z(q) - k_z(q)}{k_z(q) + \kappa_z(q)}, \\ T_1(q) &= \frac{2k_z(q)}{k_z(q) + \kappa_z(q)} \quad \text{and} \quad T_2(q) = \frac{2\kappa_z(q)}{k_z(q) + \kappa_z(q)}, \end{aligned} \quad (7)$$

where the z components of the wavevectors involved in expression (7) are defined by

$$k_z(q) = (k^2 - q^2)^{1/2} \quad \text{and} \quad \kappa_z(q) = (\kappa^2 - q^2)^{1/2} \quad (8)$$

related to the two-dimensional vector $\mathbf{q}$ that is parallel to the plane $z = 0$, and $\kappa^2 = k^2(1 + \chi)$.

The free term $E_0(\mathbf{r})$ on the right-hand side of IWE [equation (3)] can be chosen in the form

$$E_0(\mathbf{r}) = \exp(i\mathbf{q}_0\mathbf{x})y_1(z, q_0) \quad (9)$$

in accordance with the incident plane wave $E_{\mathrm{inc}}(\mathbf{r}) = \exp(i\mathbf{k}_0\mathbf{r})$.

Noteworthy is the fact that, as follows from the IWE [equation (3)], beyond the integral operators over the variables $(\mathbf{q}, \mathbf{x})$, the integration range over the variable z is determined by $\{\Theta(z) - \Theta[z - h(\mathbf{x})]\}$ and defines the behaviour of reflected and transmitted waves for $z \to \mp\infty$.

Correspondingly, the asymptotic GISAXS solutions can be cast in the form

$$\begin{aligned} E_{\mathrm{R}}(\mathbf{x}, z)|_{z\to-\infty} &= R_1(q_0)\exp[i(\mathbf{q}_0\mathbf{x} - k_z z)] \\ &\quad + \frac{i}{2\pi}\int \frac{\mathrm{d}^2\mathbf{q}}{k_z(q)}\exp[i\mathbf{q}\mathbf{x} - ik_z(q)z]A_{\mathrm{R}}(q, q_0), \\ E_{\mathrm{T}}(\mathbf{x}, z)|_{z\to\infty} &= T_1(q_0)\exp[i(\mathbf{q}_0\mathbf{x} + \kappa_z z)] \\ &\quad + \frac{i}{2\pi}\int \frac{\mathrm{d}^2\mathbf{q}}{\kappa_z(q)}\exp[i\mathbf{q}\mathbf{x} + i\kappa_z(q)z]A_{\mathrm{T}}(q, q_0) \end{aligned} \quad (10)$$

where the scattering amplitudes $A_{\mathrm{R}}(q, q_0)$ and $A_{\mathrm{T}}(q, q_0)$ are introduced as follows:

$$\begin{aligned} A_{\mathrm{R}}(\mathbf{q}, \mathbf{q}_0) &= -\frac{\chi k^2}{4\pi}\int \mathrm{d}^2\mathbf{x}_1 \exp(-i\mathbf{q}\mathbf{x}_1)\int_0^{h(\mathbf{x}_1)} \mathrm{d}z_1\, y_1(z_1, q)E(\mathbf{x}_1, z_1), \\ A_{\mathrm{T}}(\mathbf{q}, \mathbf{q}_0) &= -\frac{\chi k^2}{4\pi}\int \mathrm{d}^2\mathbf{x}_1 \exp(-i\mathbf{q}\mathbf{x}_1)\int_0^{h(\mathbf{x}_1)} \mathrm{d}z_1\, y_2(z_1, q)E(\mathbf{x}_1, z_1). \end{aligned} \quad (11)$$

Further, by using expressions (10) and (11), we will evaluate the X-ray energy flows through two planes $z \to \mp\infty$ far away from plane $z = 0$,

$$Q_{\mathrm{R}} = \frac{1}{k}\mathrm{Im}\int_S \mathrm{d}^2\mathbf{x}\left[E^*(\mathbf{x}, z)\frac{\partial}{\partial z}E(\mathbf{x}, z)\right] \text{ for } z \to -\infty, \quad (12a)$$

$$Q_{\mathrm{T}} = \frac{1}{k}\mathrm{Im}\int_S \mathrm{d}^2\mathbf{x}\left[E^*(\mathbf{x}, z)\frac{\partial}{\partial z}E(\mathbf{x}, z)\right] \text{ for } z \to \infty, \quad (12b)$$

in the explicit form, namely, one obtains

$$\begin{aligned} Q_{\mathrm{R}} &= \left[1 - |R_1(q_0)|^2\right]\frac{k_z}{k}S_2 + \frac{4\pi}{k}\mathrm{Im}\left[A_{\mathrm{R}}(\mathbf{q}_0, \mathbf{q}_0)R_1^*(q_0)\right] \\ &\quad - \frac{1}{k}\int \frac{\mathrm{d}^2\mathbf{q}}{k_z(q)}|A_{\mathrm{R}}(\mathbf{q}, \mathbf{q}_0)|^2 \end{aligned} \quad (13a)$$

and

$$\begin{aligned} Q_{\mathrm{T}} &= \exp[-2z\mathrm{Im}(\kappa_z)]|T_1(q_0)|^2\frac{\mathrm{Re}(\kappa_z)}{k}S_2 - \frac{4\pi}{k}\exp[-2z\mathrm{Im}(\kappa_z)] \\ &\quad \times \mathrm{Im}\left[A_{\mathrm{T}}(\mathbf{q}_0, \mathbf{q}_0)T_1^*(q_0)\kappa_z^*\right]\mathrm{Re}(\kappa_z^{-1}) \\ &\quad + \frac{1}{k}\int \mathrm{d}^2\mathbf{q}\,\mathrm{Re}\left[\kappa_z^{-1}(q)\right]|A_{\mathrm{T}}(\mathbf{q}, \mathbf{q}_0)|^2\exp[-2z\mathrm{Im}\kappa_z(q)] \end{aligned} \quad (13b)$$

(S_2 is an area of the reference surface illuminated by incident X-rays).

Conventionally, the optical theorem is formulated for a non-absorbing medium, $\chi^* = \chi$, putting $\overline{Q_{\mathrm{R}}} = \overline{Q_{\mathrm{T}}}$, and omitting exponentially small terms if they are on the right-hand side of equation (13b). Note that the symbol $\overline{(\ldots)}$ indicates an average procedure.

Therefore, the straightforward evaluation yields the following relationship:

$$\frac{4\pi}{k}\left\{\mathrm{Im}\left[\overline{A_{\mathrm{R}}(\mathbf{q}_0,\mathbf{q}_0)}R_1^*(q_0)\right]+T_1(q_0)\mathrm{Im}\left[\overline{A_{\mathrm{T}}(\mathbf{q}_0,\mathbf{q}_0)}\right]\Theta(q_{\mathrm{cr}}-q_0)\right\}$$
$$=\int\overline{|A_{\mathrm{R}}(\mathbf{q},\mathbf{q}_0)|^2}\,\mathrm{d}\Omega_{\mathrm{R}}+(1+\chi)^{1/2}\int\overline{|A_{\mathrm{T}}(\mathbf{q},\mathbf{q}_0)|^2}\,\mathrm{d}\Omega_{\mathrm{T}}|_{q_{\mathrm{cr}}\geq q}, \tag{14}$$

which can be interpreted as the X-ray energy conservation law in the case of the GISAXS from random rough surfaces (Kozhevnikov, 2010).

Above, the solid-angle unit elements $\mathrm{d}\Omega_{\mathrm{R}}$ and $\mathrm{d}\Omega_{\mathrm{T}}|_{q_{\mathrm{cr}}\geq q}$ ($q_{\mathrm{cr}}=k\cos\theta_{\mathrm{cr}}$)

$$\mathrm{d}\Omega_{\mathrm{R}}=\frac{\mathrm{d}^2\mathbf{q}}{kk_z(q)},\quad \mathrm{d}\Omega_{\mathrm{T}}\Big|_{q_{\mathrm{cr}}\geq q}=\frac{\mathrm{d}^2\mathbf{q}}{\kappa\kappa_z(q)} \tag{15}$$

are introduced for the scattered and transmitted beams, respectively.

The goal of the present study is to treat the issue of interest when the dimensionless parameter $k_z(q)\sigma$ is of the order of more than unity and, hence, the perturbation theory over this parameter cannot be applied to probe the optical theorem written down in the form of relationship (14).

3. The SCWA

Staying within the SCWA, where the initial X-ray wavefield is taken in the form

$$\begin{aligned}&E_{\mathrm{sc}}[\mathbf{x},z;h(\mathbf{x})]\\&=\exp(i\mathbf{q}_0\mathbf{x})\{\exp(ik_zz)+R_1(q_0)\exp[2ik_zh(\mathbf{x})-ik_zz]\}\\&\quad\text{for } z\leq h(\mathbf{x}),\\&=T_1(q_0)\exp(i\mathbf{q}_0\mathbf{x})\exp[i(k_z-\kappa_z)h(\mathbf{x})+i\kappa_zz]\\&\quad\text{for } z\geq h(\mathbf{x}),\end{aligned} \tag{16}$$

we will evaluate the scattering amplitudes $A_{\mathrm{R,T}}(\mathbf{q},\mathbf{q}_0)$ substituting equation (16) into the right-hand sides of expression (11).

Thus, the latter can be written as follows:

$$A_{\mathrm{R,T}}(\mathbf{q},\mathbf{q}_0)=\frac{i\chi k^2}{4\pi}\int\mathrm{d}^2\mathbf{x}\exp[i\mathbf{x}(\mathbf{q}_0-\mathbf{q})]Z_{\mathrm{R,T}}\big[q,q_0,h(\mathbf{x})\big], \tag{17}$$

where two non-averaged complex scattering lengths along the z direction $Z_{\mathrm{R}}[q,q_0,h(\mathbf{x})]=\int_0^{h(\mathbf{x})}\mathrm{d}z\,y_1(z,q)E_{\mathrm{sc}}(\mathbf{x},z)$ and $Z_{\mathrm{T}}[q,q_0,h(\mathbf{x})]=\int_0^{h(\mathbf{x})}\mathrm{d}z\,y_2(z,q)E_{\mathrm{sc}}(\mathbf{x},z)$ can be analytically evaluated in the explicit form, namely:

$$\begin{aligned}&Z_{\mathrm{R}}[q,q_0,h(\mathbf{x})]\\&=T_1(q)\Bigg(\frac{\exp\{i[k_z+\kappa_z(q)]h(\mathbf{x}\}-1}{k_z+\kappa_z(q)}\\&\quad+R_1(q_0)\exp[2ik_zh(\mathbf{x})]\frac{\exp\{i[-k_z+\kappa_z(q)]h(\mathbf{x})\}-1}{-k_z+\kappa_z(q)}\Bigg)\\&\quad\text{for}\quad h(\mathbf{x})\geq 0,\\&=T_1(q_0)\exp[i(k_z-\kappa_z)h(\mathbf{x})]\Bigg(\frac{\exp\{i[k_z(q)+\kappa_z]h(\mathbf{x})\}-1}{k_z(q)+\kappa_z}\\&\quad+R_1(q)\frac{\exp\{i[-k_z(q)+\kappa_z]h(\mathbf{x})\}-1}{-k_z(q)+\kappa_z}\Bigg)\\&\quad\text{for}\quad h(\mathbf{x})\leq 0\end{aligned} \tag{18a}$$

and

$$\begin{aligned}&Z_{\mathrm{T}}[q,q_0,h(\mathbf{x})]\\&=\frac{\exp\{i[k_z-\kappa_z(q)]h(\mathbf{x})\}-1}{k_z-\kappa_z(q)}+R_2(q)\frac{\exp\{i[k_z+\kappa_z(q)]h(\mathbf{x})\}-1}{k_z+\kappa_z(q)}\\&\quad+R_1(q_0)\exp[2ik_zh(\mathbf{x})]\frac{\exp\{i[-k_z-\kappa_z(q)]h(\mathbf{x})\}-1}{-k_z-\kappa_z(q)}\\&\quad+R_1(q_0)R_2(q)\exp[2ik_zh(\mathbf{x})]\frac{\exp\{i[-k_z+\kappa_z(q)]h(\mathbf{x})\}-1}{-k_z+\kappa_z(q)}\\&\quad\text{for}\quad h(\mathbf{x})\geq 0,\\&=T_2(q)T_1(q_0)\exp[i(k_z-\kappa_z)h(\mathbf{x})]\frac{\exp\{i[\kappa_z-k_z(q)]h(\mathbf{x})\}-1}{\kappa_z-k_z(q)}\\&\quad\text{for}\quad h(\mathbf{x})\leq 0.\end{aligned} \tag{18b}$$

It should be noticed that scattering lengths $Z_{\mathrm{R}}[q,q_0,h(\mathbf{x})]$ and $Z_{\mathrm{T}}[q,q_0,h(\mathbf{x})]$ as functions of scattering angle θ ($q=k\cos\theta$, $q_0=k\cos\theta_0$) reduce to zero at $\theta=0$ and $\theta=\theta_{\mathrm{cr}}$, respectively.

Formulae (14), (17) and (18*a*,*b*) represent by themselves the mathematical foundation to test the optical theorem applicability provided that an appropriate statistical average procedure of both the left-hand and right-hand sides of equation (14) will be explicitly carried out. For this, one has to specify an averaging procedure over the random rough surface and this is what we will go on to discuss in the next section.

4. Averaging procedure over the random rough surface

To evaluate the statistical averages of scattering amplitudes involved in the optical theorem relationship [equation (14)], we will utilize the following identity for averaging the fluctuating quantity $B[h(\mathbf{x})]$ (Kato, 1980; Sinha *et al.*, 1988; see also Chukhovskii, 2011)

$$\begin{aligned}&S_2^{-1}\overline{\left|\int\mathrm{d}^2\mathbf{x}\exp[i\mathbf{x}(\mathbf{q}_0-\mathbf{q})]B[h(\mathbf{x})]\right|^2}\\&=(2\pi)^2\delta_2(\mathbf{q}_0-\mathbf{q})\left|\overline{B[h(\mathbf{x})]}\right|^2\\&\quad+\left\{\overline{B[h(\mathbf{x})]B^*[h(\mathbf{x})]}-\left|\overline{B[h(\mathbf{x})]}\right|^2\right\}\\&\quad\times\int\mathrm{d}^2\mathbf{x}\exp[i\mathbf{x}(\mathbf{q}_0-\mathbf{q})]g_2(|\mathbf{x}|/\ell),\end{aligned}$$

and for simplicity the two-point cumulant correlation function $g_2(|\mathbf{x}|/\ell)$ [$g_2(0) = 1$, ℓ is the correlation length] is supposed to be isotropic varying along the distance $|\mathbf{x}|$, and it is the same for both the reflection and transmission GISAXS channels.

By applying the Gaussian statistics for a configurational average over the random rough surface and using the above identity, the straightforward evaluations yield that the Gaussian-averaged relationship [equation (14)] can be converted to

$$\left\lfloor k_z\left|R_1(q_0)\right|^2(1-f_R^2) + \kappa_z T_1^2(q_0)(1-f_T^2)\Theta(q_{cr}-q_0)\right\rfloor = \frac{\chi^2 k^2}{(4\pi)^2}\int d^2\mathbf{q}\left[\frac{\eta_R(q,q_0)}{k_z(q)} + \frac{\eta_T(q,q_0)}{\kappa_z(q)}\Theta(q_{cr}-q_0)\right] \times \int d^2\mathbf{x}\exp[i\mathbf{x}(\mathbf{q}_0-\mathbf{q})]g_2(|\mathbf{x}|/\ell), \quad (19)$$

where the statistical scattering factors $\eta_R(\theta,\theta_0)$ and $\eta_T(\theta,\theta_0)$ ($q = k\cos\theta$, $q_0 = k\cos\theta_0$) are defined as

$$\eta_R(q,q_0) = k^2\left[\overline{Z_R(q,q_0,h)Z_R^*(q,q_0,h)} - \left|\overline{Z_R(q,q_0,h)}\right|^2\right],$$
$$\eta_T(q,q_0) = k^2\left[\overline{Z_T(q,q_0,h)Z_T^*(q,q_0,h)} - \left|\overline{Z_T(q,q_0,h)}\right|^2\right] \quad (20)$$

and the conventional Debye–Waller factors are equal to

$$f_R = \exp(-2k_z^2\sigma^2), \quad f_T = \exp[-0.5(k_z-\kappa_z)^2\sigma^2], \quad (21)$$

respectively.

Before proceeding further let us consider relationship (19) in the case of infinite correlation lengths $\ell \to \infty$.

In the case of $\ell \to \infty$ the two-point cumulant correlation function $g_2(|\mathbf{x}|/\ell)$ is equal to unity for any given distance $|\mathbf{x}|$.

Then, it is easy to show that equation (19) reduces to

$$2\left\lfloor k_z\left|R_1(q_0)\right|^2(1-f_R) + \kappa_z T_1^2(q_0)(1-f_T)\Theta(q_{cr}-q_0)\right\rfloor = \frac{\chi^2 k^4}{4}\left[\frac{1}{k_z}\overline{Z_R(q_0,q_0,h)Z_-^*(q_0,q_0,h)} + \frac{1}{\kappa_z}\overline{Z_T(q_0,q_0,h)Z_+^*(q_0,q_0,h)}\Theta(q_{cr}-q_0)\right]. \quad (22)$$

Furthermore, using the explicit expressions for the Gaussian-averaged scattering-length squares involved in equation (22),

$$\overline{Z_R(q_0,q_0,h)Z_R^*(q_0,q_0,h)} = \frac{8k_z^2|R_1|^2}{\chi^2 k^4}(1-f_R),$$
$$\overline{Z_T(q_0,q_0,h)Z_T^*(q_0,q_0,h)} = \frac{8\kappa_z^2 T_1^2}{\chi^2 k^4}(1-f_T), \quad (23)$$

which relate to both the diffuse reflection and transmission GISAXS channels, respectively, we can immediately obtain that relationship (22) turns to identity.

In other words, we come to an assertion that the optical theorem within the SCWA is strictly carried out in the case of infinite correlation lengths $\ell \to \infty$.

In general, in the case of finite correlation lengths ℓ, in order to numerically test the optical theorem some Gaussian averages are required. In particular, the straightforward calculations yield the following expressions {for reference, $\overline{\exp[i(\alpha-\alpha^*)h]\Theta(h)} = 0.5\exp[-0.5(\alpha-\alpha^*)^2\sigma^2] \times \mathrm{Erfc}[-i(\alpha-\alpha^*)\sigma/2^{1/2}]$}:

$$\begin{aligned}
&\overline{Z_R(q,q_0,h)Z_R^*(q,q_0,h)}\\
&= 0.5\left|a_R\right|^2\{\exp[-0.5(\alpha-\alpha^*)^2\sigma^2]\mathrm{Erfc}[-i(\alpha-\alpha^*)\sigma/2^{1/2}]\\
&\quad - 2\mathrm{Re}[\exp(-0.5\alpha^2\sigma^2)\mathrm{Erfc}(-i\alpha)\sigma/2^{1/2}] + 1\}\\
&+ 0.5\left|b_R\right|^2\{\exp[-0.5(\beta-\beta^*)^2\sigma^2]\mathrm{Erfc}[-i(\beta-\beta^*)\sigma/2^{1/2}]\\
&\quad - 2\mathrm{Re}[\exp(-0.5\beta^2\sigma^2)\mathrm{Erfc}(-i\beta)\sigma/2^{1/2}] + 1\}\\
&+ \mathrm{Re}(a_R b_R^*\{\exp[-0.5\sigma^2(\alpha-\beta^*-\gamma)^2]\\
&\quad \times \mathrm{Erfc}[-i(\alpha-\beta^*-\gamma)\sigma/2^{1/2}]\\
&\quad - \exp[-0.5\sigma^2(\alpha-\gamma)^2]\mathrm{Erfc}[-i(\alpha-\gamma)\sigma/2^{1/2}]\\
&\quad - \exp[-0.5\sigma^2(\beta^*+\gamma)^2]\mathrm{Erfc}[i(\beta^*+\gamma)\sigma/2^{1/2}]\\
&\quad + \exp(-0.5\sigma^2\gamma^2)\mathrm{Erfc}(i\gamma\sigma/2^{1/2})\})\\
&+ 0.5\left|c_R\right|^2\{\exp[-0.5\sigma^2(\mu+\zeta-\zeta^*-\mu^*)^2]\\
&\quad \times \mathrm{Erfc}[i(\mu+\zeta-\zeta^*-\mu^*)\sigma/2^{1/2}]\\
&\quad - \exp[-0.5\sigma^2(\mu+\zeta-\zeta^*)^2]\mathrm{Erfc}[i(\mu+\zeta-\zeta^*)\sigma/2^{1/2}]\\
&\quad - \exp[-0.5\sigma^2(\zeta-\zeta^*-\mu^*)^2]\mathrm{Erfc}[i(\zeta-\zeta^*-\mu^*)\sigma/2^{1/2}]\\
&\quad + \exp[-0.5\sigma^2(\zeta-\zeta^*)^2]\mathrm{Erfc}[i(\zeta-\zeta^*)\sigma/2^{1/2}]\}\\
&+ 0.5\left|d_R\right|^2\{\exp[-0.5\sigma^2(\nu+\zeta-\zeta^*-\nu^*)^2]\\
&\quad \times \mathrm{Erfc}[i(\nu+\zeta-\zeta^*-\nu^*)\sigma/2^{1/2}]\\
&\quad - \exp[-0.5\sigma^2(\nu+\zeta-\zeta^*)^2]\mathrm{Erfc}[i(\nu+\zeta-\zeta^*)\sigma/2^{1/2}]\\
&\quad - \exp[-0.5\sigma^2(\zeta-\zeta^*-\nu^*)^2]\mathrm{Erfc}[i(\zeta-\zeta^*-\nu^*)\sigma/2^{1/2}]\\
&\quad + \exp[-0.5\sigma^2(\zeta-\zeta^*)^2]\mathrm{Erfc}[i(\zeta-\zeta^*)\sigma/2^{1/2}]\}\\
&+ \mathrm{Re}(c_R d_R^*\{\exp[-0.5\sigma^2(\mu+\zeta-\zeta^*-\nu^*)^2]\\
&\quad \times \mathrm{Erfc}[i(\mu+\zeta-\zeta^*-\nu^*)\sigma/2^{1/2}]\\
&\quad - \exp[-0.5\sigma^2(\mu+\zeta-\zeta^*)^2]\mathrm{Erfc}[i(\mu+\zeta-\zeta^*)\sigma/2^{1/2}]\\
&\quad - \exp[-0.5\sigma^2(\zeta-\zeta^*-\nu^*)^2]\mathrm{Erfc}[i(\zeta-\zeta^*-\nu^*)\sigma/2^{1/2}]\\
&\quad + \exp[-0.5\sigma^2(\zeta-\zeta^*)^2]\mathrm{Erfc}[i(\zeta-\zeta^*)\sigma/2^{1/2}]\}) \quad (24a)
\end{aligned}$$

and

$$\begin{aligned}
&\left|\overline{Z_R(q,q_0,h)}\right|^2\\
&= 0.25|a_R[\exp(-0.5\alpha^2\sigma^2)\mathrm{Erfc}(-i\alpha\sigma/2^{1/2}) - 1]\\
&+ b_R\{\exp[-0.5(\beta+\gamma)^2\sigma^2]\mathrm{Erfc}[-i(\beta+\gamma)\sigma/2^{1/2}]\\
&\quad - \exp(-0.5\gamma^2\sigma^2)\mathrm{Erfc}(-i\gamma\sigma/2^{1/2})\}\\
&+ c_R\{\exp[-0.5(\mu+\zeta)^2\sigma^2]\mathrm{Erfc}[i(\mu+\zeta)\sigma/2^{1/2}]\\
&\quad - \exp(-0.5\zeta^2\sigma^2)\mathrm{Erfc}(i\zeta\sigma/2^{1/2})\}\\
&+ d_R\{\exp[-0.5(\nu+\zeta)^2\sigma^2]\mathrm{Erfc}[i(\nu+\zeta)\sigma/2^{1/2}]\\
&\quad - \exp(-0.5\zeta^2\sigma^2)\mathrm{Erfc}(i\zeta\sigma/2^{1/2})\}|^2, \quad (24b)
\end{aligned}$$

$$
\begin{aligned}
&\overline{Z_{\rm T}(q,q_0,h)Z_{\rm T}^*(q,q_0,h)}\\
&=(|a_{\rm T}|^2+|c_{\rm T}|^2)|a_{\rm T}|^2\{1-{\rm Re}[\exp(-0.5\sigma^2\alpha^2){\rm Erfc}(-i\alpha\sigma/2^{1/2})]\}\\
&+(|b_{\rm T}|^2+|d_{\rm T}|^2)\{1-{\rm Re}[\exp(-0.5\sigma^2\beta^2){\rm Erfc}(-i\beta\sigma/2^{1/2})]\}\\
&+|e_{\rm T}|^2(\exp[-0.5\sigma^2(\zeta-\zeta^*+\nu-\nu^*)^2]{\rm Erfc}[i(\zeta-\zeta^*+\nu-\nu^*)\sigma/2^{1/2}]\\
&\quad-2{\rm Re}\{\exp[-0.5\sigma^2(\nu+\zeta-\zeta^*)^2]{\rm Erfc}[i(\nu+\zeta-\zeta^*)\sigma/2^{1/2}]\}\\
&\quad+\exp[-0.5\sigma^2(\zeta-\zeta^*)^2]{\rm Erfc}[i(\zeta-\zeta^*)\sigma/2^{1/2}])\\
&+{\rm Re}(a_{\rm T}b_{\rm T}^*\{\exp[-0.5(\alpha+\beta)^2\sigma^2]{\rm Erfc}[-i(\alpha+\beta)\sigma/2^{1/2}]\\
&\quad-\exp(-0.5\alpha^2\sigma^2){\rm Erfc}(-i\alpha\sigma/2^{1/2})\\
&\quad-\exp(-0.5\beta^2\sigma^2){\rm Erfc}(i\beta\sigma/2^{1/2})+1\})\\
&+{\rm Re}(a_{\rm T}c_{\rm T}^*\{\exp[-0.5(2\alpha-\gamma)^2\sigma^2]{\rm Erfc}[-i(2\alpha-\gamma)\sigma/2^{1/2}]\\
&\quad-2\exp[-0.5(\alpha-\gamma)^2\sigma^2]{\rm Erfc}[-i(\alpha-\gamma)\sigma/2^{1/2}]\\
&\quad+\exp(-0.5\gamma^2\sigma^2){\rm Erfc}(i\gamma\sigma/2^{1/2})\})\\
&+{\rm Re}(a_{\rm T}d_{\rm T}^*\{\exp[-0.5(\alpha-\beta-\gamma)^2\sigma^2]{\rm Erfc}[-i(\alpha-\beta-\gamma)\sigma/2^{1/2}]\\
&\quad-\exp[-0.5(\alpha-\gamma)^2\sigma^2]{\rm Erfc}[-i(\alpha-\gamma)\sigma/2^{1/2}]\\
&\quad-\exp[-0.5(\beta+\gamma)^2\sigma^2]{\rm Erfc}[i(\beta+\gamma)\sigma/2^{1/2}]\\
&\quad+\exp(-0.5\gamma^2\sigma^2){\rm Erfc}(i\gamma\sigma/2^{1/2})\})\\
&+{\rm Re}(b_{\rm T}c_{\rm T}^*\{\exp[-0.5(\alpha-\beta-\gamma)^2\sigma^2]{\rm Erfc}[-i(\alpha-\beta-\gamma)\sigma/2^{1/2}]\\
&\quad-\exp[-0.5(\beta+\gamma)^2\sigma^2]{\rm Erfc}[i(\beta+\gamma)\sigma/2^{1/2}]\\
&\quad-\exp[-0.5(\alpha-\gamma)^2\sigma^2]{\rm Erfc}[-i(\alpha-\gamma)\sigma/2^{1/2}]\\
&\quad+\exp(-0.5\gamma^2\sigma^2){\rm Erfc}(i\gamma\sigma/2^{1/2})\})\\
&+{\rm Re}(b_{\rm T}d_{\rm T}^*\{\exp[-0.5(2\beta+\gamma)^2\sigma^2]{\rm Erfc}[i(2\beta+\gamma)\sigma/2^{1/2}]\\
&\quad-2\exp[-0.5(\beta+\gamma)^2\sigma^2]{\rm Erfc}[i(\beta+\gamma)\sigma/2^{1/2}]\\
&\quad+\exp(-0.5\gamma^2\sigma^2){\rm Erfc}(i\gamma\sigma/2^{1/2})\})\\
&+{\rm Re}(c_{\rm T}d_{\rm T}^*\{\exp[-0.5(\alpha+\beta)^2\sigma^2]{\rm Erfc}[i(\alpha+\beta)\sigma/2^{1/2}]\\
&\quad-\exp(-0.5\alpha^2\sigma^2){\rm Erfc}(i\alpha\sigma/2^{1/2})\\
&\quad-\exp(-0.5\beta^2\sigma^2){\rm Erfc}(i\beta\sigma/2^{1/2})+1\}) \qquad (25a)
\end{aligned}
$$

and

$$
\begin{aligned}
&\left|\overline{Z_{\rm T}(q,q_0,h)}\right|^2\\
&=0.25|a_{\rm T}[\exp(-0.5\alpha^2\sigma^2){\rm Erfc}(-i\alpha\sigma/2^{1/2})-1]\\
&+b_{\rm T}[\exp(-0.5\beta^2\sigma^2){\rm Erfc}(i\beta\sigma/2^{1/2})-1]\\
&+c_{\rm T}\{\exp[-0.5(\alpha-\gamma)^2\sigma^2]{\rm Erfc}[i(\alpha-\gamma)\sigma/2^{1/2}]\\
&\quad-\exp(-0.5\gamma^2\sigma^2){\rm Erfc}(-i\gamma\sigma/2^{1/2})\}\\
&+d_{\rm T}\{\exp[-0.5(\beta+\gamma)^2\sigma^2]{\rm Erfc}[-i(\beta+\gamma)\sigma/2^{1/2}]\\
&\quad-\exp(-0.5\gamma^2\sigma^2){\rm Erfc}(-i\gamma\sigma/2^{1/2})\}\\
&+e_{\rm T}\{\exp[-0.5(\nu+\zeta)^2\sigma^2]{\rm Erfc}[i(\nu+\zeta)\sigma/2^{1/2}]\\
&\quad-\exp(-0.5\zeta^2\sigma^2){\rm Erfc}(i\zeta\sigma/2^{1/2})\}|. \qquad (25b)
\end{aligned}
$$

Herein, the complementary error function $\mathrm{Erfc}[w]$ for the complex argument w is introduced. Correspondingly, the array $\{\alpha, \beta, \gamma, \mu, \nu, \zeta\}$ with z-component wavevector combinations

$$
\begin{aligned}
&\alpha = k_z + \kappa_z(q), \quad \beta = -k_z + \kappa_z(q), \quad \gamma = 2k_z,\\
&\mu = k_z(q) + \kappa_z, \quad \nu = -k_z(q) + \kappa_z, \quad \zeta = k_z - \kappa_z \qquad (26)
\end{aligned}
$$

and two arrays $\{a_{\rm R}, b_{\rm R}; c_{\rm R}, d_{\rm R}\}$, $\{a_{\rm T}, b_{\rm T}, c_{\rm T}, d_{\rm T}; e_{\rm T}\}$ with amplitudes of the partial scattering lengths related to both the reflection and transmission GISAXS channels

$$
\begin{aligned}
&a_{\rm R} = T_1(q)/\alpha, \quad b_{\rm R} = T_1(q)R_1(q_0)/\beta;\\
&c_{\rm R} = T_1(q_0)/\mu, \quad d_{\rm R} = T_1(q_0)R_1(q)/\nu, \qquad (27a)
\end{aligned}
$$

$$
\begin{aligned}
&a_{\rm T} = R_2(q)/\alpha, b_{\rm T} = -R_2(q)/\beta, c_{\rm T} = -R_1(q_0)/\alpha,\\
&d_{\rm T} = R_1(q_0)R_2(q)/\beta; e_{\rm T} = T_2(q)T_1(q_0)/\nu \qquad (27b)
\end{aligned}
$$

are determined by equations (27a) and (27b), respectively.

To complete the statistical description of a random rough surface, we will choose the explicit expression for the two-point cumulant correlation function as $g_2(|\mathbf{x}|/\ell) = \exp(-|\mathbf{x}|/\ell)$.

Then, in this case, the Fourier transform of the two-point cumulant correlation function as chosen takes the form

$$
\begin{aligned}
g_2(\mathbf{q}-\mathbf{q}_0) &\equiv \int {\rm d}^2\mathbf{x}\exp[i(\mathbf{q}_0-\mathbf{q})]g_2(|\mathbf{x}|\ell)\\
&= \frac{2\pi\ell^2}{\left[1+\ell^2(\mathbf{q}_0-\mathbf{q})^2\right]^{3/2}}. \qquad (28)
\end{aligned}
$$

5. Numerical run-through for probing the optical theorem

Before proceeding further, additional comments are appropriate concerning some of the theoretical aspects of implementing the SCWA.

If it would appear that the r.m.s. roughness $\sigma \times \max[|\alpha|, |\beta|, \gamma, |\mu|, |\nu|, |\zeta|]$ is smaller than unity, a consequent analysis shows that the statistical scattering factors [equation (20)] reduce to $\sigma^2|T_1(q)|^2|T_1(q_0)|^2 + 0(\sigma^3)$, $\sigma^2|T_2(q)|^2|T_1(q_0)|^2 + 0(\sigma^3)$, respectively, for reflection and transmission, and then the SCWA matches the first-order perturbation theory calculations based on the Fresnel eigenfunctions in their regime of validity for the diffuse GISAXS (Vinogradov *et al.*, 1985).

In general, the above theoretical formulae (20), (21) and (24a,b)–(28) have to be summed and substituted in equation (19) to numerically probe the optical theorem for the typical-valued $\{\theta_0, \sigma, \ell\}$ parameters of interest.

We now present results of numerical calculations to clarify how the optical theorem works for finite correlation lengths.

As examples, using expression (20) along with (24a,b)–(27a,b) the statistical scattering factors $\eta_{\rm R}(\theta, \theta_0)$ and $\eta_{\rm T}(\theta, \theta_0)$ *versus* the grazing scattering angle $\theta/\theta_{\rm cr}$ are numerically computed for the r.m.s. roughness $k\sigma = 200$ and two values of the grazing-incidence angle $\theta_0/\theta_{\rm cr}$ ($\theta_0/\theta_{\rm cr} = 2$ in Fig. 2 and 3 in Fig. 3).

It is seen that the statistical scattering factors $\eta_{\rm R}(\theta, \theta_0)$ depicted in Figs. 2(a) and 3(a) have narrow maxima very close to the value of $\theta/\theta_{\rm cr} = 1$, proving the diffuse GISAXS scan peak experimentally observed (see Yoneda, 1963; Vinogradov *et al.*, 1985; Chukhovskii, 2011 for details). As may be seen, the factor $\eta_{\rm R}(\theta, \theta_0)$ has a peak height that for $\theta_0/\theta_{\rm cr} = 2$ (Fig. 2a) is two times more than the corresponding peak height for $\theta_0/\theta_{\rm cr} = 3$ (Fig. 3a).

In contrast to the factors $\eta_{\rm R}(\theta, \theta_0)$, the statistical scattering factors $\eta_{\rm T}(\theta, \theta_0)$ depicted in Figs. 2(b) and 3(b) have equal-height peaks at the scattering angle θ value close to the inci-

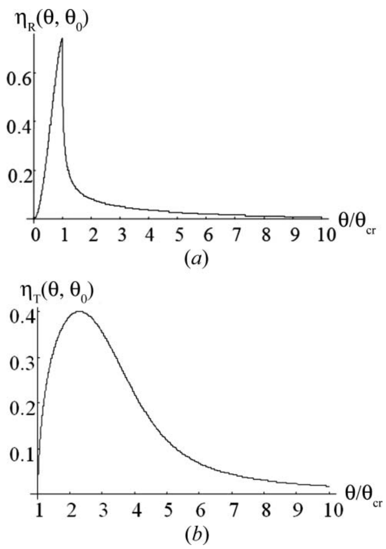

Figure 2
Gaussian-averaged statistical scattering factors $\eta_R(\theta, \theta_0)$ (*a*) and $\eta_T(\theta, \theta_0)$ (*b*) (scaled $\times 10^{-5}$) for the r.m.s. roughness $k\sigma$ = 200 and the grazing-incidence angle θ_0/θ_{cr} = 2.

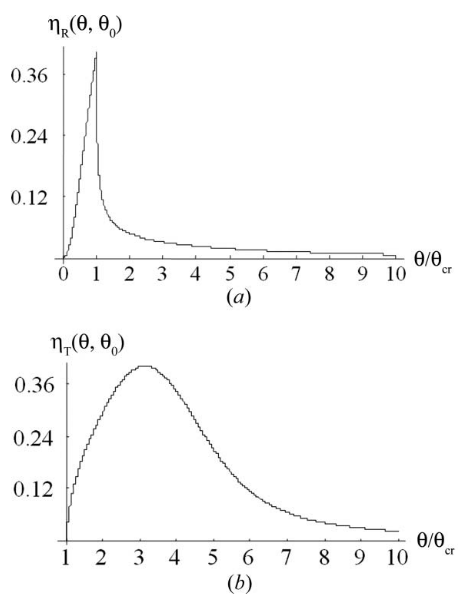

Figure 3
Gaussian-averaged statistical scattering factors $\eta_R(\theta, \theta_0)$ (*a*) and $\eta_T(\theta, \theta_0)$ (*b*) (scaled $\times 10^{-5}$) for the r.m.s. roughness $k\sigma$ = 200 and the grazing-incidence angle θ_0/θ_{cr} = 3.

dent angle, $\theta/\theta_0 \geq 1$, with a slight variation in the peak-to-tail ratio and peak width.

Note that the peak widths of the statistical scattering factors $\eta_T(\theta, \theta_0)$ related to the transmission GISAXS channel are much larger than the peak widths of the corresponding peaks of the factors $\eta_R(\theta, \theta_0)$ related to the reflection GISAXS channel (*cf.* Figs. 2*a*, 2*b* and Figs. 3*a*, 3*b*).

To probe the optical theorem applicability within the SCWA for finite correlation lengths $k\ell$, $k\ell \gg 1$, we will integrate the right-hand side of equation (19) over the entire angular range (θ, φ), using the Fourier transform of the two-point cumulant correlation function as chosen in equation (28).

Table 1
The computed FOF values as calculated from equation (19) for the grazing-incidence angles θ_0/θ_{cr}: (*a*) = 0.5, (*b*) = 2, (*c*) = 3.

	$k\sigma$	
$k\ell$	100	200
(*a*)		
10^5	0.54543	0.53162
10^6	0.16252	0.15725
10^7	0.02261	0.02244
(*b*)		
10^5	0.10426	0.16047
10^6	0.00065	0.01068
10^7	0.00006	0.00099
(*c*)		
10^5	0.02972	0.10872
10^6	0.00118	0.01103
10^7	0.00004	0.00105

Taking into account that the azimuth angles φ which contribute to integrating the right-hand side of equation (19) are of the order of $(k\ell\theta_0)^{-1} \ll 1$, the corresponding integration over the variable φ can be analytically carried out.

Furthermore, the simple trapezium algorithm that we used has been applied for numerical integration of the right-hand side of equation (19) over the angular variable θ. The numerical integration step chosen is equal to $2 \times 10^{-3}\theta_{cr}$.

The input data were the grazing-incidence angles of θ_0/θ_{cr} = {0.5, 2, 3}, the r.m.s. roughness of $k\sigma$ = {100, 200} and the correlation lengths of $k\ell$ = {10^5, 10^6, 10^7}.

The numerical results of testing the optical theorem within the SCWA are listed in Table 1.

How well the optical theorem works can be gauged by introducing a figure of feasibility (FOF), which can be defined as FOF = |diffuse terms − specular terms|/specular terms, at the end of calculating all the terms related to the specular (the left-hand side) and diffuse (the right-hand side) components of equation (19).

For reference, each side of equation (19) contains two terms related to the reflection and transmission GISAXS channels. Clearly, the small values of FOF, for instance, when the FOFs are less than 0.01, do mean that the optical theorem is satisfied within an accuracy up to 1%.

Being dependent on the correlation length values of $k\ell$, the optical theorem within the SCWA seems to work well provided that the FOF reaches a value much smaller than unity.

Ultimately, as seen from Table 1, in the case of $k\ell = 10^7$, $k\ell\theta_0^2 \gg 1$, the FOF values are rather small for all the input data under consideration and, therefore, the optical theorem works well even for θ_0/θ_{cr} = 0.5, *i.e.* in the case when the incident angles are below the critical angle of the total reflection region. Loosely speaking, the present study shows that the infinite correlation length case [equation (22)] is realized in practice under the condition $k\ell\theta_0^2 \gg 1$.

6. Concluding remarks

The study presented here supports the key idea regarding the optical theorem applicability within the SCWA. A rigorous description of the X-ray wavefield propagation through the twofold medium has been based on the IWE [equation (3)] adjusted with the Green function formalism and a statistical Gaussian model of a random rough surface using the two-point cumulant correlation function $g_2(|\mathbf{x}|/\ell)$. Unlike in the DWBA method, to determine the adequate asymptotic solutions of the non-averaged IWE [equation (3)] we have used the SCWA for the initial X-ray wavefield approach. It has allowed us to formulate the optical theorem beyond the small effective values of the r.m.s. roughness σ.

The present treatment of the optical theorem is based on the two physical prerequisites mathematically pointed out in Chukhovskii (2011). Let us briefly repeat them. One of them is applying the SCWA to search asymptotic solutions of the non-averaged IWE [equation (3)] using the initial continuous wavefield in a self-consistent sense near a rough surface. Another is applying the Gaussian-averaged isotropic surface model in terms of the r.m.s. roughness σ and correlation length ℓ.

A combination of both these assumptions along with Fourier transform of the two-point cumulant correlation function as defined by equation (28) has allowed us to numerically test the optical theorem applicability for some range of the GISAXS parameters.

By using the SCWA, the analytical expressions for statistical scattering factors $\eta_{\rm R}(\theta,\theta_0)$ and $\eta_{\rm T}(\theta,\theta_0)$ of the diffuse components of the reflection and transmission GISAXS have been obtained for the Gaussian-averaged surfaces in terms of the r.m.s. roughness σ and correlation length ℓ. These statistical scattering factors multiplied by the Fourier transform of the two-point cumulant correlation function have been used for a numerical run-through to probe the optical theorem for some correlation lengths $k\ell = \{10^5, 10^6, 10^7\}$ and grazing-incidence angles $\theta_0/\theta_{\rm cr} = \{0.5, 2, 3\}$. It is shown that the optical theorem applicability within the SCWA becomes effective under the condition $k\ell\theta_0^2 \gg 1$.

The questions of how and whether the optical theorem within the SCWA works and whether it has any validity in cases where the two-point cumulant correlation function differs from expression (28) should be developed anew.

One point remains constant, namely: in the limit of infinite correlation lengths, $k\ell \to \infty$, for any shape of the two-point cumulant correlation function and, hence, any type of random rough surface the optical theorem within the SCWA does strictly hold.

Valuable discussions with I. V. Kozhevnikov, A. M. Polyakov and S. V. Salikhov are gratefully acknowledged. S. V. Salikhov is thanked for rendering Fig. 1.

References

Boer, D. K. G. de (1994). *Phys. Rev. B Condens. Matter*, **49**, 5817–5823.
Boer, D. K. G. de (1995). *Phys. Rev.* **51**, 5297–5302.
Chukhovskii, F. N. (2009). *Acta Cryst.* A**65**, 39–45.
Chukhovskii, F. (2011). *Acta Cryst.* A**67**, 200–209.
Chukhovskii, F. N. & Polyakov, A. M. (2010). *Acta Cryst.* A**66**, 640–648.
Kato, N. (1980). *Acta Cryst.* A**36**, 763–769.
Kozhevnikov, I. V. (2010). *Crystallogr. Rep.* **55**, 539–545.
Lazzari, R. (2002). *J. Appl. Cryst.* **35**, 406–421.
Nevot, L. & Croce, P. (1980). *Rev. Phys. Appl.* **15**, 761–779.
Petrashen', P. V., Kov'ev, E. K., Chukhovskii, F. N. & Degtyarev, Yu. L. (1983). *Solid State Phys.* **25**, 1211–1214.
Pietsch, U., Holy, V. & Baumbach, T. (2004). *High-Resolution X-ray Scattering – From Thin Films to Lateral Nanostructures.* Berlin: Springer Verlag.
Renaud, G., Lazzari, R. & Leroy, F. (2009). *Surf. Sci. Rep.* **64**, 255–380.
Schmidbauer, M., Schäfer, P., Besedin, S., Grigoriev, D., Köhler, R. & Hanke, M. (2008). *J. Synchrotron Rad.* **15**, 549–557.
Sinha, S. K., Sirota, E. B., Garoff, S. & Stanley, H. B. (1988). *Phys. Rev. B*, **38**, 2297–2311.
Vinogradov, A. V., Zorev, N. N., Kozhevnikov, I. V. & Yakushkin, I. G. (1985). *Sov. Phys. JETF*, **62**, 1225–1233.
Yoneda, Y. (1963). *Phys. Rev.* **131**, 2010–2013.
Zozulya, A. V., Yefanov, O. M., Vartanyants, I. A., Mundboth, K., Mocuta, C., Metzger, T. H., Stangl, J., Bauer, G., Böck, T. & Schmidbauer, M. (2008). *Phys. Rev. B*, **78**, 121304.